

## Article

# Distributed Cooperative Jamming with Neighborhood Selection Strategy for Unmanned Aerial Vehicle Swarms

Yongkun Zhou <sup>1</sup>, Dan Song <sup>2</sup>, Bowen Ding <sup>1</sup>, Bin Rao <sup>1</sup>, Man Su <sup>3</sup> and Wei Wang <sup>1,\*</sup>

<sup>1</sup> The School of Electronics and Communication Engineering, Sun Yat-Sen University, Guangzhou 510000, China; zhouyk6@mail2.sysu.edu.cn (Y.Z.); dingbw@mail2.sysu.edu.cn (B.D.); raob@mail.sysu.edu.cn (B.R.)

<sup>2</sup> The College of Information and Communication, National University of Defense Technology, Xi'an 710000, China; dansong91@hotmail.com

<sup>3</sup> The Beijing Institute of Tracking and Telecommunication Technology, Beijing 100000, China; suman\_bcng@163.com

\* Correspondence: wangw278@mail.sysu.edu.cn

**Abstract:** In system science, a swarm possesses certain characteristics which the isolated parts and the sum do not have. In order to explore emergence mechanism of a large-scale electromagnetic agents (EAs), a neighborhood selection (NS) strategy-based electromagnetic agent cellular automata (EA-CA) model is proposed in this paper. The model describes the process of agent state transition, in which a neighbor with the smallest state difference in each sector area is selected for state transition. Meanwhile, the evolution rules of the traditional CA are improved, and performance of different evolution strategies are compared. An application scenario in which the emergence of multi-jammers suppresses the radar radiation source is designed to demonstrate the effect of the EA-CA model. Experimental results show that the convergence speed of NS strategy is better than those of the traditional CA evolution rules, and the system achieves effective jamming with the target after emergence. It verifies the effectiveness and prospects of the proposed model in the application of electronic countermeasures (ECM).

**Keywords:** unmanned aerial vehicle (UAV); electromagnetic agent cellular automata (EA-CA) model; neighborhood selection (NS); electronic countermeasures (ECM)



**Citation:** Zhou, Y.; Song, D.; Ding, B.; Rao, B.; Su, M.; Wang, W. Distributed Cooperative Jamming with Neighborhood Selection Strategy for Unmanned Aerial Vehicle Swarms. *Electronics* **2022**, *11*, 184. <https://doi.org/10.3390/electronics11020184>

Academic Editor: Gerardo Di Martino

Received: 22 November 2021

Accepted: 1 January 2022

Published: 7 January 2022

**Publisher's Note:** MDPI stays neutral with regard to jurisdictional claims in published maps and institutional affiliations.



**Copyright:** © 2022 by the authors. Licensee MDPI, Basel, Switzerland. This article is an open access article distributed under the terms and conditions of the Creative Commons Attribution (CC BY) license (<https://creativecommons.org/licenses/by/4.0/>).

## 1. Introduction

The unmanned aerial vehicle (UAV) has gradually gained popularity in the last few years. In the beginning, UAVs were mainly used for military purposes, and now they are increasingly appearing in the fields of industry and academic research. In terms of autonomous flight research of UAVs, [1] proposes the development of a camera-based quadrotor positioning system to finish the process of automated landing. Reference [2] studies the autonomous navigation system for small UAVs suitable for GPS-denied environment, and realizes the collision-free navigation in fully autonomous missions. The state feedback linear quadratic regulator (LQR) controller is applied to the quadrotor UAV to realize the complete autonomy of the control system [3].

Due to limitations of the load and battery capacity of a single UAV, it is difficult to complete some tasks in complex environments. In recent years, UAV swarms have developed rapidly due to their potential huge application value [4]. UAV swarms show the group behavior through the local interaction between individuals, to solve the global collaborative task [5]. Meanwhile, the current trend of electronic countermeasures (ECM) is moving towards intelligent and distributed direction. Compared with traditional centralized ECM, distributed ECM takes advantage of its number and space to achieve better jamming with targets [6]. The background of distributed ECM and the key technical challenges can be referred to in [7]. In [8], the influence of distributed suppression and deception jamming

on radar detection performance is studied. It investigates the jamming effect of a dense UAV swarm on the detection performance of air defense radar. The optimization for the position of each individual through sparse array synthesis is addressed in [9]. However, these studies only demonstrate the effectiveness of distributed ECM, and there is still a lack of corresponding theoretical modeling for analysis on the evolution mechanism of distributed ECM.

The cellular automata (CA) has been used to model the propagation and emergence of cluster behavior in complex systems [10]. The traditional modeling method is based on the differential equations and is studied by deductive reasoning, while the CA model simulates and predicts the overall dynamic process. The CA model has been widely used in many fields such as computer network modeling and communication [11–13]. In the computer field, the side profile flow calculation of sand-like particles in video games is researched in [11]. The CA model can also be used to model computer networks [12]. Reference [13] studies a node scheduling algorithm based on CA, which saves the energy of sensor nodes while ensuring communication coverage. However, there is no literature addressing the application of CA in the field of ECM.

Given these gaps in this research, the main contributions of this paper are summarized as follows:

(a) The process of agent state transition is explored, in which the all selection (AS) strategy of the traditional CA model is improved based on the neighborhood selection (NS) strategy; (b) On the basis of (a), the convergence performance of the model in the four evolution strategies is analyzed; (c) Electromagnetic agents (EA) are UAVs that carry electronic reconnaissance or jamming equipment. By regarding each as a cell, the electromagnetic agent-cellular automata (EA-CA) model is proposed. It is used to simulate the process of cluster jamming in distributed ECM scenarios; (d) By adjusting the parameters of the simulation, the conditions for the system to realize the emergence jamming are analyzed.

The rest of this paper is organized as follows: Section 2 describes the state transition process of CA based on the neighborhood selection-all selection (NS-AS) strategy. The application of the EA-CA model under ECM scenario is introduced in Section 3. In Section 4, the performance of the model and the ECM simulation results are provided to demonstrate the effectiveness of proposed model. Concluding remarks are given in Section 5.

## 2. The EA-CA Model

### 2.1. Mechanism of EA-CA

The definition of CA is described based on the set theory as follows: Denote the dimension of the cell space as  $d$ , the neighbor radius of the cell as  $r$ , and time as  $t$ . The cell state is a value in the finite state set  $S$ , and  $Z$  is a set of integers in one dimension. In distributed ECM scenarios, two-dimensional CA [14] are commonly used for modeling. The state of a cell at the next moment is determined by the current states of its neighboring cells. Thus, the state value of a cell at  $t$  can be summarized as

$$S_{i,j}^t = f(S_{i,j}^{t-1}, S_{i-1,j}^{t-1}, S_{i+1,j}^{t-1}, S_{i-1,j-1}^{t-1}, S_{i-1,j+1}^{t-1}, S_{i,j-1}^{t-1}, S_{i,j+1}^{t-1}, S_{i+1,j+1}^{t-1}, S_{i+1,j-1}^{t-1}) \quad (1)$$

Let  $G(V, E, A)$  represent the diagram of communication topology structure of the CA model. The elements in the set  $V = 1, 2, \dots, n$  are used to mark the corresponding  $n$  agent members in turn, and the state of agent  $i$  is denoted by  $x_i(t)$ . The set of communication edges between members is represented by  $E = \{(i, j) : i, j \in V, i \neq j\}$ .

According to the rules of CA, the consensus algorithm [15] of the system can be defined as

$$\dot{x}_i(t) = - \sum_{i,j \in E} a_{ij}(t) (x_j(t) - x_i(t)) \quad (2)$$

where  $a_{ij}$  is an element of the adjacency matrix  $A(t) = [a_{ij}(t)]$  at  $t \geq 0$ . The weight assigned to the edge of the graph  $G$  is defined as

$$(i, j) \in E \iff a_{ij} > 0, (i, j) \notin E \iff a_{ij} = 0, a_{ii} = 0 \tag{3}$$

Then, the adjacency matrix  $A$  represents the communication network between all agents in the system. Given that  $G$  is an undirected graph, the degree of the agent  $i$  is

$$d(i) = d_{in}(i) = d_{out}(i) = \sum_{j=1}^n a_{ji} \tag{4}$$

and the degree matrix can be denoted by  $D = \text{diag}\{d(i), i \in V\}$ ; the elements of  $D$  can be written as

$$d_i = \begin{cases} \sum_{j=1}^n a_{ji}, & i = j \\ 0, & i \neq j \end{cases} \tag{5}$$

Combining Formulas (3) and (5), the Laplacian matrix of the figure  $G$  can be obtained by  $L = D - A$ . The element of  $L, l_{ij}$ , is given by

$$L = [l_{ij}](i, j = 1, 2, \dots, n) = \begin{cases} \sum_{j=1}^n a_{ij}, & i = j \\ -a_{ij}, & i \neq j \end{cases} \tag{6}$$

The consensus algorithm of the system based on CA can be written in matrix form  $\dot{x} = -Lx, x = [x_1, x_2, \dots, x_n]$ . It can be seen from the evolutionary rules of CA that the state of each agent is determined by the states of its neighbors. Therefore, when  $t \rightarrow \infty$  and  $|x_i(t) - x_j(t)| \rightarrow 0$ , the system achieves global consistency, i.e., the states of all agents converge to a common value.

### 2.2. The NS-AS Strategy

The traditional CA model adopts the AS strategy, i.e., the state of agent is determined by the states of all its neighboring agents. This makes the system more computationally-consumed and difficult to converge, while using the NS strategy can increase the convergence speed of the system and improve the stability of the system [16,17]. In the NS strategy, neighboring agents are divided into several communication sectors. In order to benefit the system convergence and enhance the system consistency, the neighbor agents with the smallest state difference in each communication sector are selected to construct the backbone network topology. In the network topology, all candidate neighbor agents of agent  $i$  participate in the calculation of the state update for agent  $i$ . Thus, the state transition equation is given by

$$x_i(t + 1) = x_i(t) + u_i(t) \tag{7}$$

where  $u_i(t)$  represents the control input. Supposing a neighborhood member  $j$  with the smallest state difference between the communication area and that of the agent  $i$ , the agent  $i$  selects the agent  $j$  for collaborative cooperation and adds it to the candidate set. Then,  $u_i(t)$  can be written as

$$u_i(t) = \alpha \left( \sum_{u=1}^m (x_{\min(i^u)}(t) - x_i(t)) + \sum_{ii \in P_i(t), ii \notin A_i(t)} (x_{ii}(t) - x_i(t)) \right) \tag{8}$$

where  $\alpha$  is the adjustment factor of the model,  $m$  represents the number of communication sector,  $i^u$  represents the neighbor agents set of agent  $i$  in the  $u$ th sector, and  $x_{\min(i^u)}(t)$  is the state of the agent with smallest difference from the state of agent  $i$  among its neighboring agents in the  $u$ th sector at time  $t$ . In the above,  $P_i(t)$  and  $A_i(t)$  represent the set of

neighborhood members of agent  $i$  and the set of agents from the smallest state difference in each sector, respectively.

As the NS strategy only selects the neighbor agent with the smallest difference in each sector to participate in the update calculation, a small sum of state difference is obtained. The step of each update of the agent is small, which causes the system to converge too slowly. Therefore, in order to improve the convergence speed of the system, the system switches to the NS-AS strategy. When the system is fully connected, the number of neighbor agents of agent  $i$  is  $n - 1$ , and all agents within communication range are select to participate in state evolution. The algorithm process of the NS-AS strategy is shown in Algorithm 1.

---

**Algorithm 1:** The NS-AS Strategy Algorithm

---

The NS-AS strategy for  $n$  agents:

- 1: Initialize the network topology and  $x_i(t), i \in 1, 2 \dots N$
  - 2: for agent  $i=1$  to  $N$
  - 3:   if the network is not fully connected
  - 4:     Adopt the NS steategy
  - 5:     Divide the agents into several communication sectors.
  - 6:     Calculate the rotation angle set  $\beta = rotate\_array(min(std(N_n)))$
  - 7:     for  $j = 1$  to  $m$
  - 8:       Selects the neighbor agent  $\min(i^u) = argmin||x_{iu}(t) - x_i(t)||$ ,  
add the agent into candidate set  $u_i(t)$ , update  $x_i(t)$ ;
  - 9:        $\exists ii, ii \in P_i(t), ii \notin A_i(t)$ , add agent  $ii$  into candidate set  $u_i(t)$ ;
  - 10:       Acoording to candidate set  $u_i(t)$ , update  $x_i(t)$ .
  - 11:     end for
  - 12:   else
  - 13:     Switch to AS strategy
  - 14:     Select all agents in the neighborhood, update  $x_i(t)$
  - 15:   end for
- 

By calculating the standard deviation of the number of agents in each sector, the angle of the rotating sector can be adjusted. In Algorithm 1, *rotate\_array* represents the list of rotation angles to be searched, which cannot exceed the angle of each sector.  $N_n$  represents the number of agents in each sector and  $N_c$  denotes the number of communication sector.

Combining Formulas (11) and (12), the state information of agent can be set as

$$\begin{aligned} &\forall i, N_i(t) < n - 1 : \\ x_i(t + 1) = &x_i(t) + \alpha 1 \left\{ \sum_{u=1} x_{\min(i^u)}(t) - x_i(t) \right. \\ &+ \left. \sum_{ii \in P_i(t), ii \notin A_i(t)} (x_{ii}(t) - x_i(t)) \right\}; \end{aligned} \tag{9}$$

$$\begin{aligned} &\forall i, N_i(t) = n - 1 : \\ x_i(t + 1) = &x_i(t) + \alpha 2 \sum_{j \in N_i(t)} (x_j(t) - x_i(t)). \end{aligned} \tag{10}$$

where  $N_i$  represents the number of neighbor agents of agent  $i$ , and  $\alpha 1$  and  $\alpha 2$  represent the adjustment factor in different condition, respectively.

### 3. Signal Model of ECM

The EA-CA model can be used to simulate the process of agent state transition in ECM application scenarios. The jamming consistency to radiation sources can be achieved through the information interaction between agents [18]. In order to realize the distributed

noise suppression jamming with the radar [7], each jammer is regarded as an electromagnetic agent that transmits jamming noise that drowns the echo of a radar-detected target.

The radar detection equation without jamming can be written as [19]

$$P_r = \frac{P_t G_t G_r(\theta_t) \delta \lambda^2 K_I K_C}{(4\pi)^3 R^4 L_s} \quad (11)$$

where  $P_t$  and  $G_t$  correspond to the transmitting power and the gain of the transmitting antenna, respectively.  $G_r(\theta_t)$  is the gain of the radar antenna in the target direction,  $\delta$  is the radar cross section,  $\lambda$  is the wavelength of signal, and  $K_I$  and  $K_C$  represent the pulse accumulation correction factor and the pulse compression correction factor, respectively. In the above,  $R$  is the distance between radar and target.  $L_s$  is the signal transmission loss in clear air; Appendix A the definition of mathematical symbols, Appendix B gives the specific calculation process.

The noise power of the system contains the thermal noise power of the receiver and the jamming noise power. The thermal noise power can be written as  $P_{rn} = kT_0 B_r F_n$ , where  $k$  is Boltzmann constant, and  $T_0$  is the standard room temperature.  $B_r$  is radar receiver bandwidth, and  $F_n$  is noise figure.

The jamming signal power of  $n$  jammers received by the radar is represented as follows [20]

$$P_{rj} = \sum_{i=1}^n \frac{P_j G_j G_r(\theta_j) \lambda^2}{(4\pi)^2 R_j^2 L_j} \cdot \frac{B_r}{B_j} \quad (12)$$

where  $P_j$  and  $G_j$  represent the jammer power and gain.  $G_r(\theta_j)$  is the gain of radar antenna in the direction of jammer, and  $R_j$  denotes the distance and loss of the jammer, of which  $B_r$  and  $B_j$  stand for the bandwidth of receiver and jammer, respectively.

The total noise power of the system is given by  $P_n = P_{rn} + P_{rj}$  [6]. The total signal-noise ratio (SNR) of the system can be expressed as follows:

$$\left(\frac{S}{N}\right)_s = \frac{P_r}{P_n} = \frac{P_t G_r(\theta_t) \delta \lambda^2 K_I K_C}{(4\pi)^3 R^4 L_s (kT_0 B_r F_n + P_{rj})} \quad (13)$$

In practice, it draws more attention to SNR or detection probability of the radar receiver. For a radar receiver,  $(SNR)_{o\min}$  is the minimum output SNR [21]. The minimum detectable signal power is

$$S_{i\min} = kT_0 B_r F_n (SNR)_{o\min} \quad (14)$$

The detection probability is related to false alarm probability  $P_{fa}$ , output SNR  $(SNR)_o$ , and the type of target fluctuation. The detection probability of a non-undulating target [22] can be calculated approximately by

$$P_d = 0.5 \operatorname{erfc}\left(\sqrt{-\ln(P_{fa})} - \sqrt{(SNR)_o + 0.5}\right). \quad (15)$$

where  $\operatorname{erfc}()$  represents the complementary error function.

## 4. Simulation Results Analysis

### 4.1. Performance Analysis of the EA-CA Model

The EA-CA model is evaluated in a simulated scenario. The initial topology in the EA-CA model is connected. When an EA detects the radiation source, it transmits the information to its neighboring agents and the neighborhood agents transform their states from the reconnaissance state to the jamming state. The evolution process of the EA state information in different strategies is shown in Figure 1. The color keys in the figure indicate the evolution of each agent state. In the ECM scenarios, state Y represents the state of agent with the initial state being reconnaissance state. When the radiation source is detected, the agent state evolves to the jamming state with the increase of reconnaissance information. The performances of different evolution strategies are determined by final convergence

or divergence. It can be seen that when the AS strategy is adopted, the communication topology of the EA–CA model is not always connected during the evolution process, and the system will converge to multiple local centers. The NS strategy 1 represents dividing the neighboring agent into several sectors. The NS strategy 2 is based on the NS strategy 1, by adjusting the angle of the sectors to make the individuals of each sector evenly distributed. When using the NS strategy 1, the communication area of each agent is divided into several sectors, and the communication topology is always connected during the evolution process. The EA–CA model converges to a small area quickly, then to achieve the consensus at a very slow speed. When the NS strategy 2 is adopted, the number of agents in each sector is evenly distributed, and its convergence speed is faster than the NS strategy 1. When the communication topology of the model has not reached full connectivity, the system adopts NS strategy 2, and the convergence speed at this time is closed to the NS strategy 2. When the communication topology of the model reaches full connectivity, it switches to AS strategy; the convergence speed at this time is faster than NS strategy 2.

The influence of different parameters, such as the number of communication sectors, the communication radius of agent, the number of agents, and the different adjustment factors on the convergence speed of the system are also analyzed.

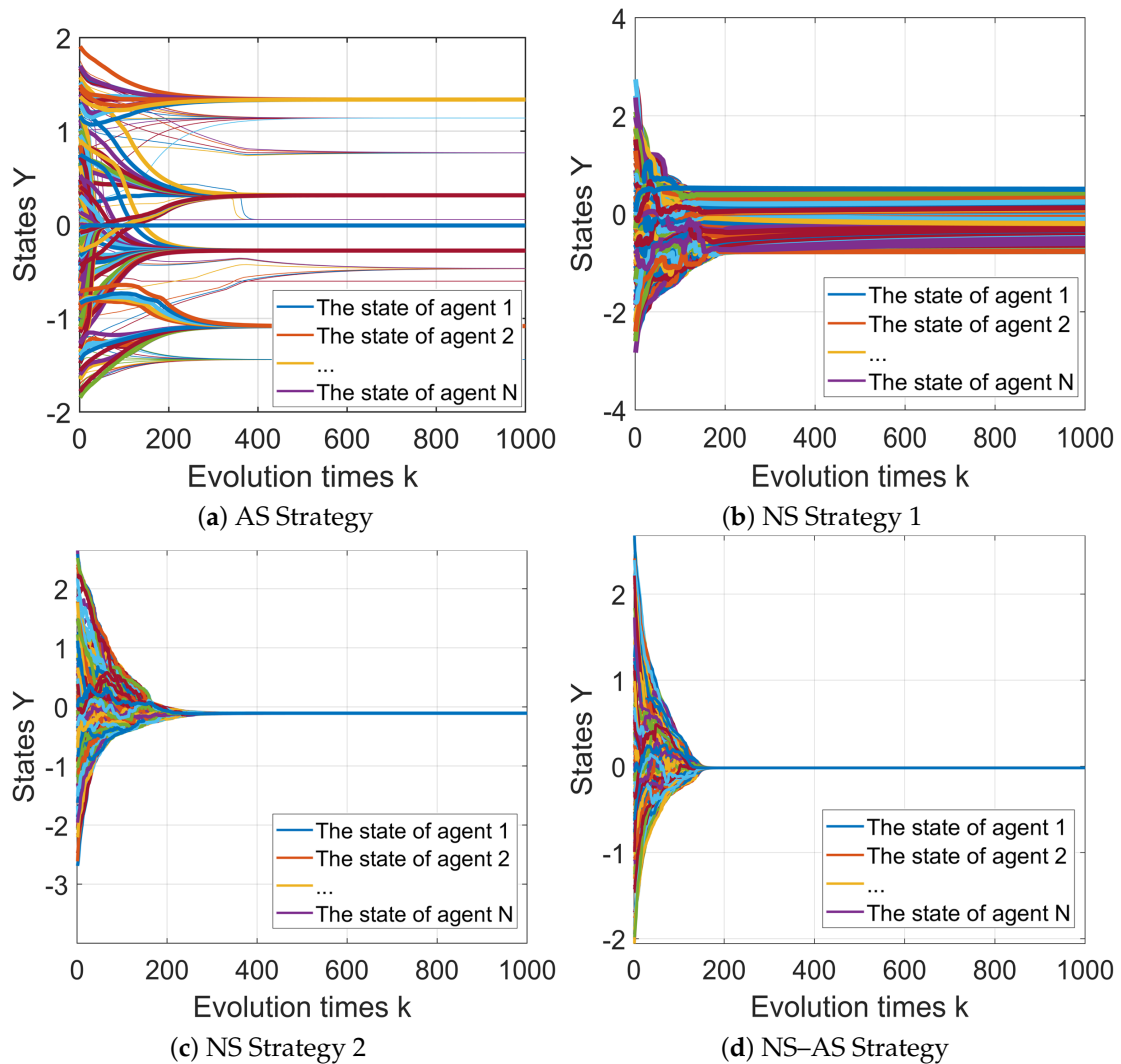


Figure 1. The evolution process of EA–CA model state information in different strategies.

#### 4.1.1. The Number of Communication Sector

The evolutions of state using NA–AS strategy with the different number of communication sectors are shown in Figure 2. The number of agents in the candidate set decreases when the number of sectors is too small, which leads to the system converge to multiple local centers. If the number of sectors is set too large, though the convergence speed can be improved, the computational cost increases.

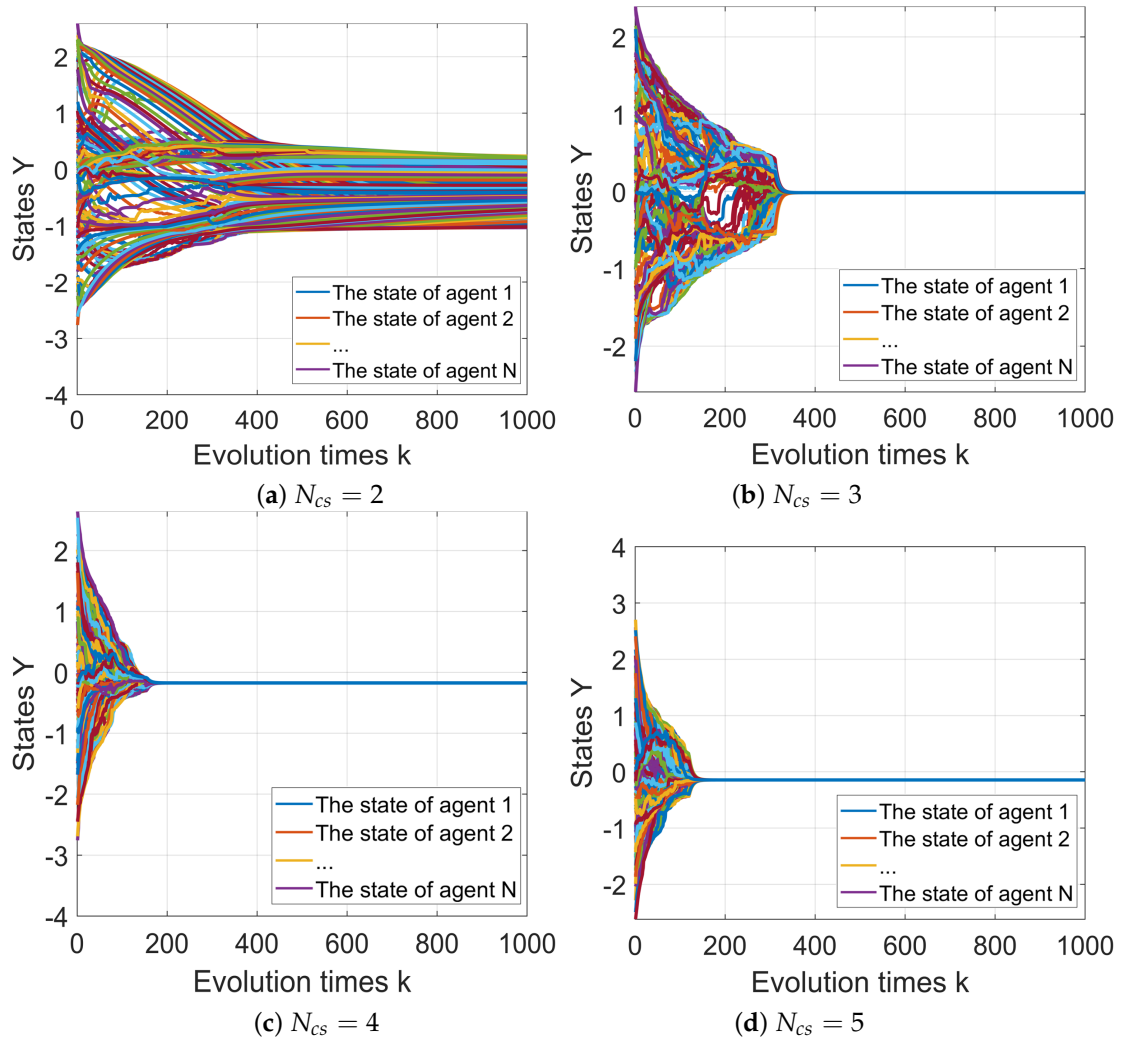


Figure 2. The evolution performance with the number of different sectors.

#### 4.1.2. The Communication Radius of the Agent

Figure 3 shows the evolutions of state using NA–AS strategy with different communication radius. It can be seen that the number of candidate agents is positively correlated with the size of communication radius, so the convergence speed of the system increases accordingly. The number of neighbor agents decreases when the communication radius is too small, which causes divergence.

#### 4.1.3. The Number of the Agents

The evolutions of state using NA–AS strategy with the different number of agents are observed in Figure 4. The system converge speed is related with the density of agents, the system diverges to multiple statuses when the number of agents is small. However, a large number of agents leads to the increase of the computation cost, resulting in a slow converge speed.

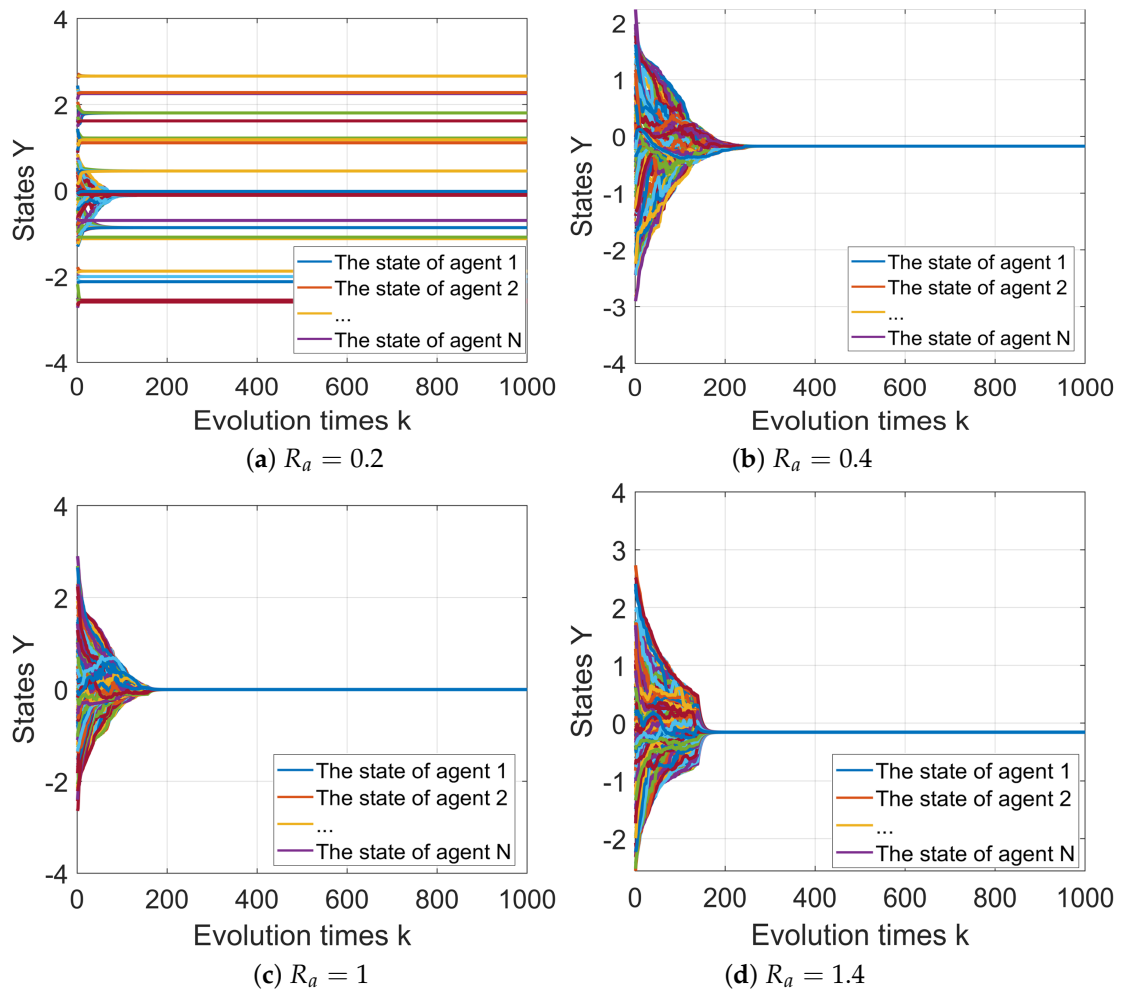


Figure 3. The evolution performance with different communication radius.

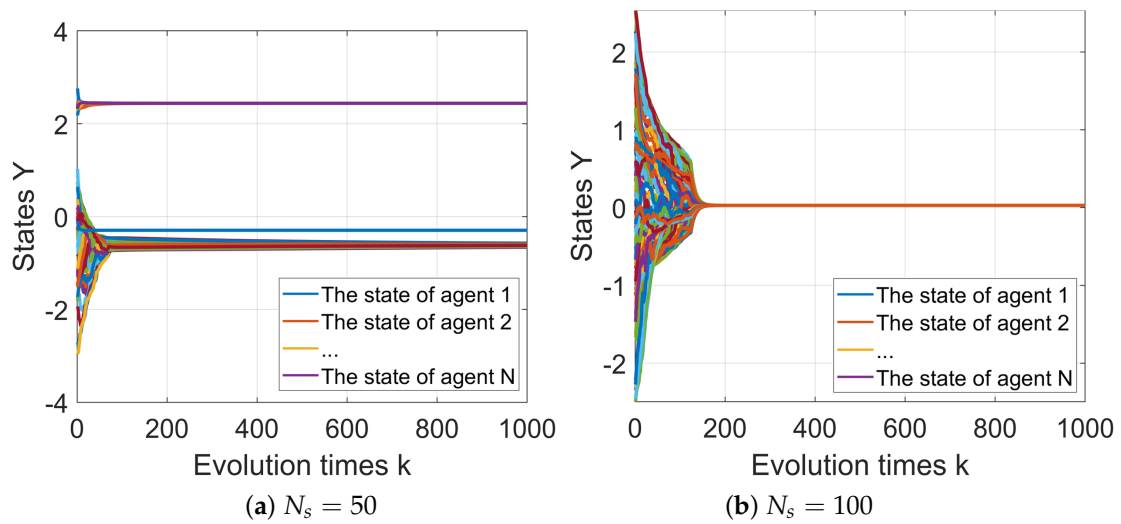


Figure 4. Cont.

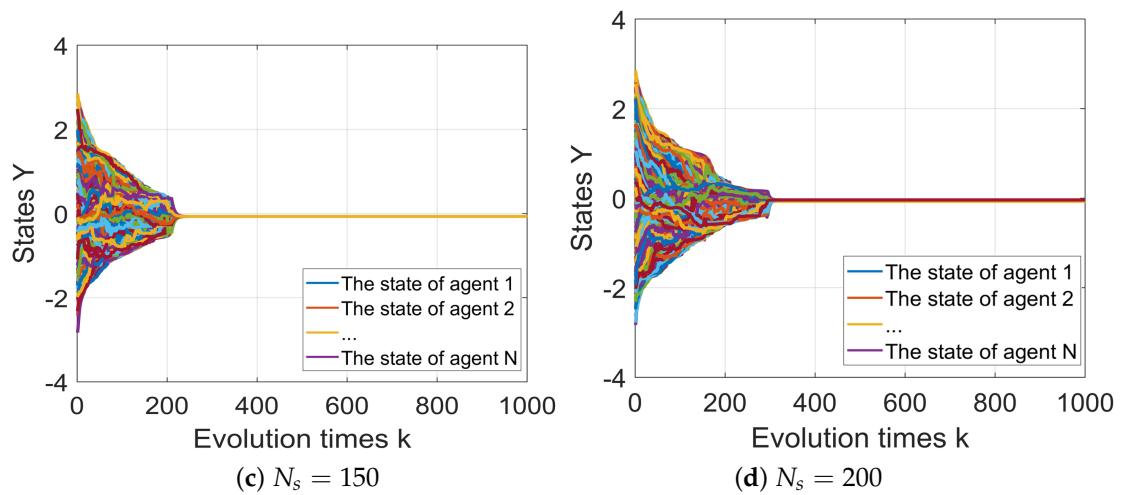


Figure 4. The evolution performance with the different number of agents.

4.1.4. The Adjustment Factor

Figure 5 shows the effect of different adjustment factors on the system convergence performance. Adjustment factor denotes the step-step process of the agent state change. The unreasonable adjustment factor set may cause the modeled divergence.

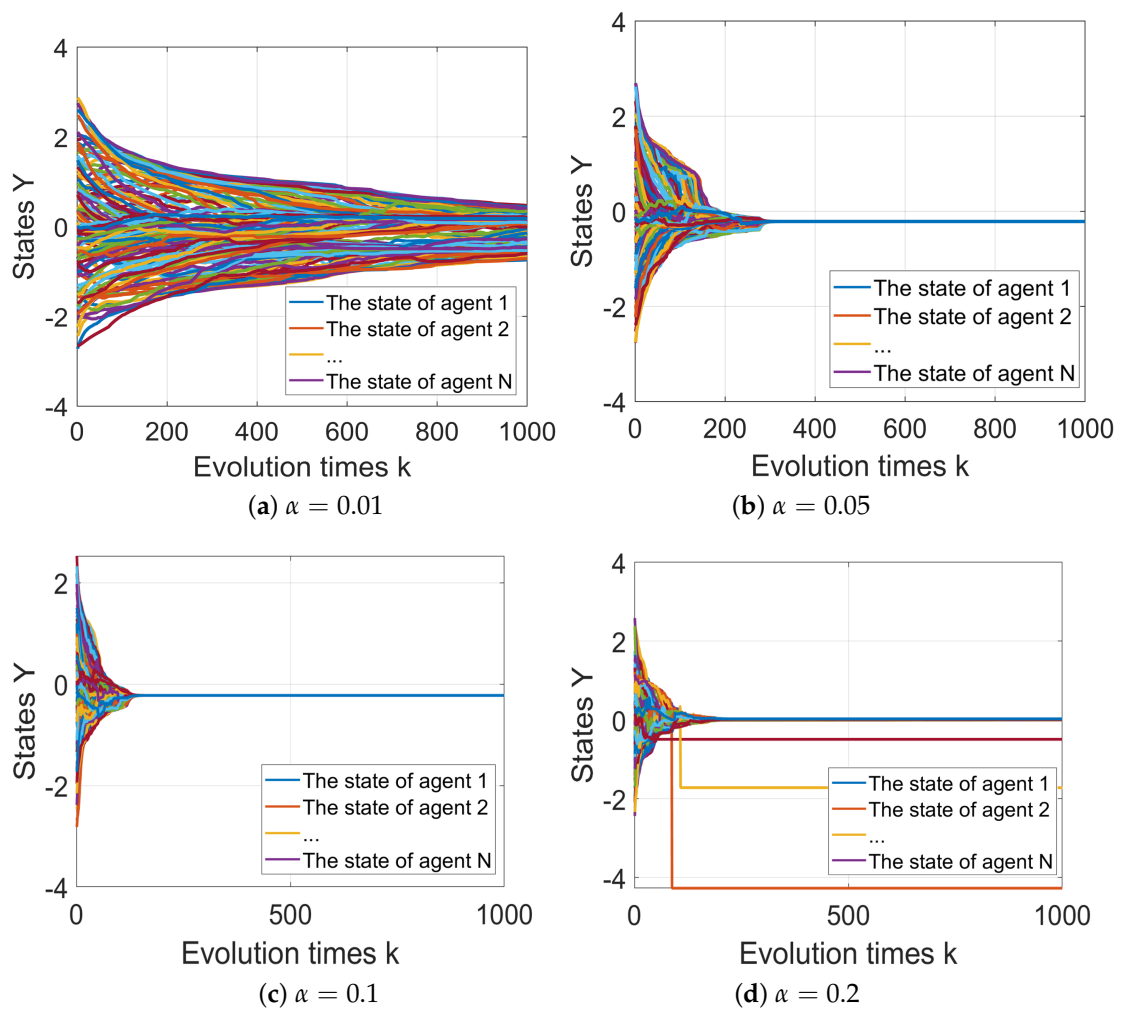


Figure 5. The evolution performance with different  $\alpha$ .

### 4.2. ECM Simulation Results

#### 4.2.1. ECM Simulated Scenario

An ECM simulated scenario is shown in Figure 6. Each UAV carries reconnaissance and jamming payloads. When the radar radiation source is detected, it will perform jamming, covering the target. The relevant parameters with their values are shown in Table 1.

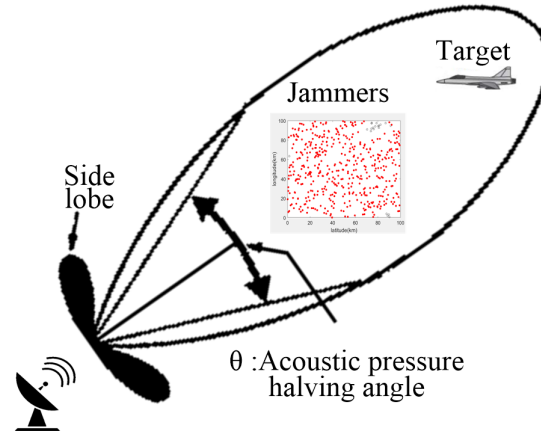


Figure 6. The ECM scenario based on UAV swarm.

Table 1. Simulation parameters with their values.

Parameter	Definition	Value
$F_r$	The radar center frequency	3.1 GHz
$T_r$	The pulse width	20 $\mu$ s
$B_w$	The chirp bandwidth	30 MHz
$B_r$	The bandwidth of receiver	100 MHz
$G_r$	The antenna gain of radar in the jammer direction	38.5 dB
$B_j$	The bandwidth of jammer	50 MHz
$P_j$	The jammer transmitting power	3 W
$G_j$	The jammer transmitting antenna gain	20 dB
$L_j$	The comprehensive loss of jammer	5 dB

The jamming pattern of this paper is noise convolutional jamming signal. The jamming signal  $S_j$  is formed by the convolution of the received radar signal  $S_r$  and the Gaussian white noise signal  $S_n$ . The jamming signal can be represented as follows:

$$S_j = conv(S_r, S_n) \tag{16}$$

$$S_r = exp(j\pi Kt^2) \tag{17}$$

where  $exp()$  is the exponential function with the constant  $e$  as the base, and  $K = B_w/T_r$  is the frequency modulation slope.

The time domain and frequency domain of jamming signal are shown in Figure 7.

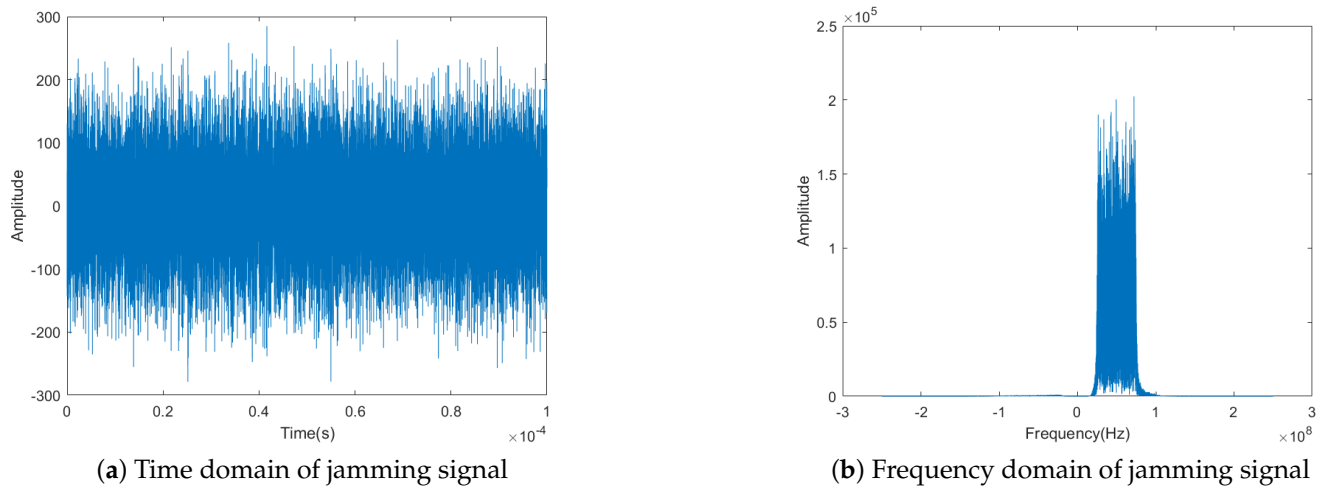


**Figure 7.** Time domain and frequency domain of the jamming signal.

#### 4.2.2. The Performance Analysis of Different Evolution Strategies

Figure 8 shows the radar detection power map of a single radar interfered with by multiple jammers. When the main lobe of the radar antenna points to the direction of jammer distribution, multiple jammers effectively suppress the radar exposure area.

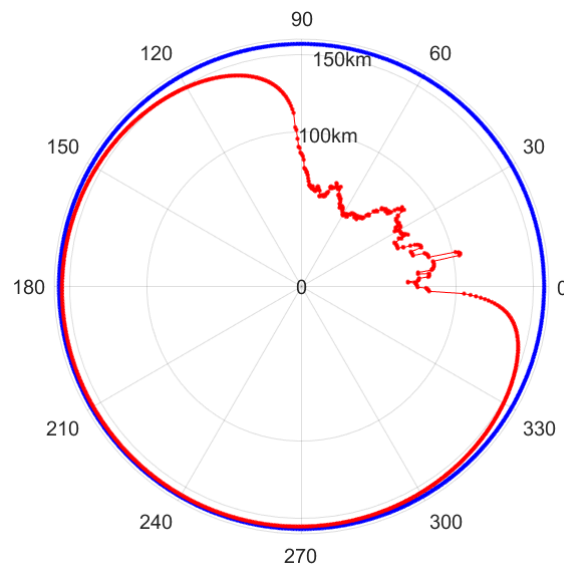


**Figure 8.** Radar detection power map.

In order to verify the influence of the number of jammers on the performance of the radar, the relationship between the number of UAVs and the signal-to-noise ratio of the system is shown in Figure 9. As the evolution process progresses, the number of UAVs in jamming state gradually increases, and the signal-to-noise ratio of the system decreases accordingly.

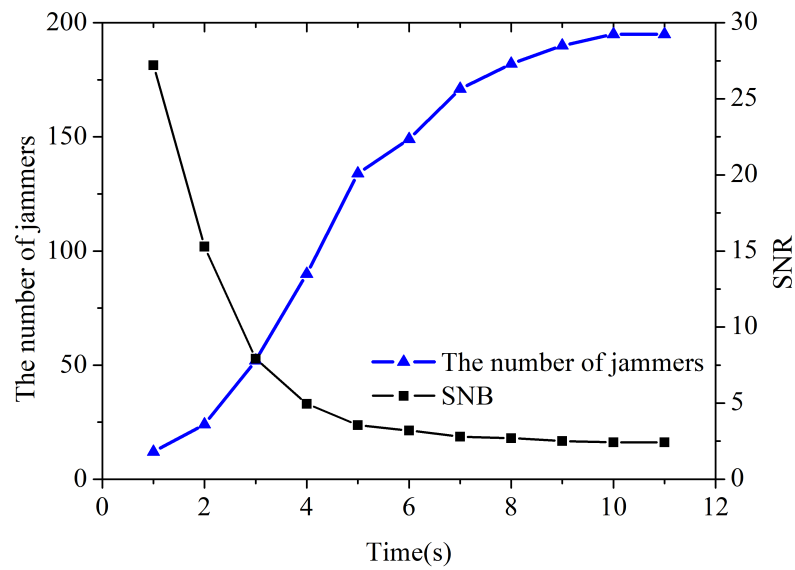


Figure 9. The influence of the number of jammers on the system SNR.

The curve of the radar target detection probability with different number of jammers is shown in Figure 10. The detection probabilities under various jammer transmit power are compared. In an actual scenario, the number of jammers and the jamming power should be considered comprehensively. The experimental results show that to optimally allocate jamming resources, the number of jammers and the interference power can be adjusted according to actual application requirements.

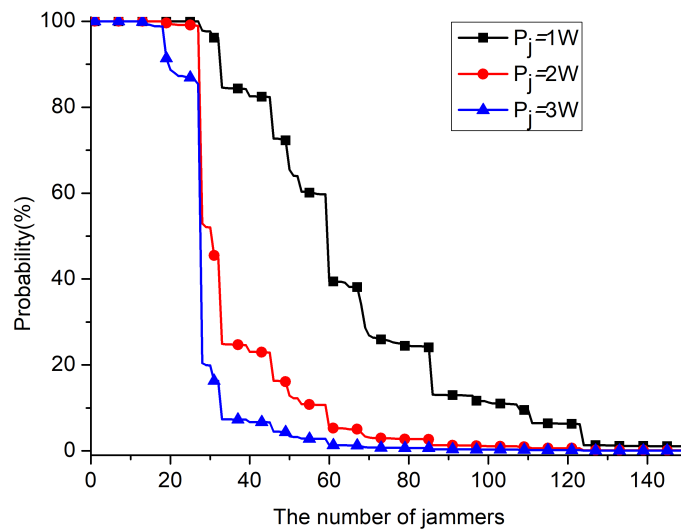


Figure 10. The curve of the radar target detection probability.

Figure 11 shows the influence of different evolution strategies on the radar detection probability. It can be seen that as the evolution progresses, the number of UAVs in the jamming state gradually increases, and the radar detection probability gradually decreases. From the previous analysis results, the AS strategy and NS strategy 1 converge to multiple local centers with only certain individuals evolving to the interference state. Due to the lack of sufficient interference power, these two strategies cannot effectively interfere with the radar. On the contrary, both NS strategy 2 and NS-AS strategy can eventually achieve effective interference with the radar. Meanwhile, as the convergence speed of the NS-AS strategy is faster than the NS strategy 2, it achieves effective interference faster.

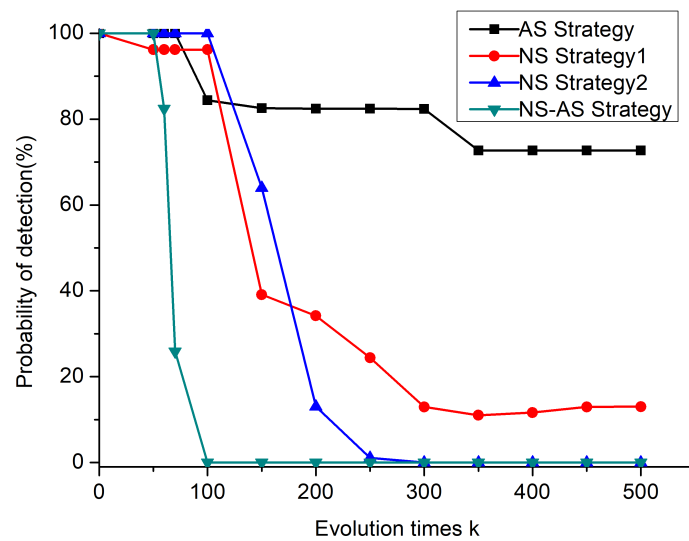


Figure 11. The influence of different evolution strategies on the radar detection probability.

When radar performs the searching and tracking task, it usually uses pulse compression technology to improve the target detection capabilities. The effect of a few jammers on the radar pulse compression output is described in Figure 12. It can be seen that as the evolution process progresses, the number of UAVs in the jamming state gradually increases, and the radar detection probability gradually decreases. The target echo is detected normally when the SNR is large in Figure 12a. However, with the constant transition of the agent state, more agents are transformed into the jamming state. As can be seen in Figure 12b, the target echo submerges into background noise with the jamming power increasing. It verifies the effectiveness of the interference signal by comparing the results of pulse pressure output under different signal-to-noise ratios.

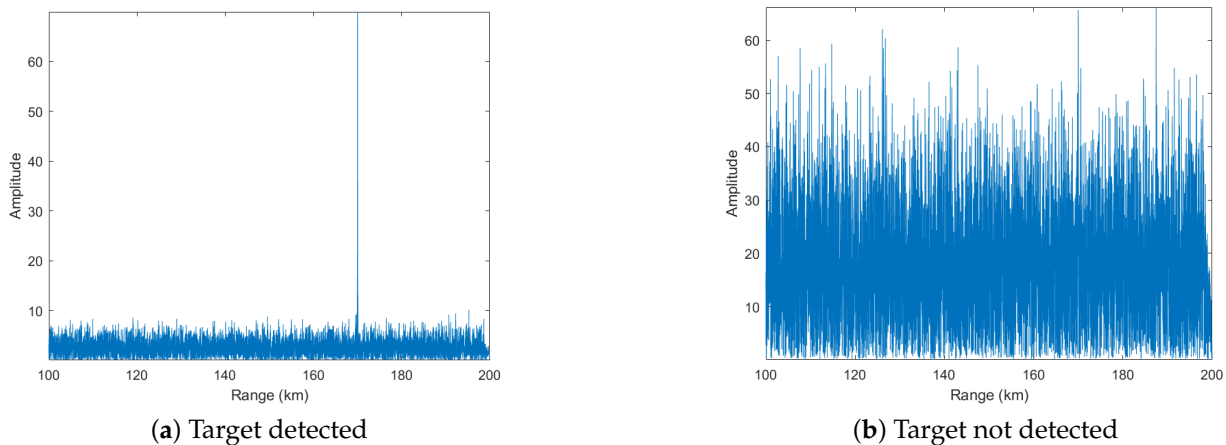


Figure 12. Target detection results after radar pulse compression.

### 5. Conclusions

In this paper, an EA-CA model based on NS strategy was proposed, and the effectiveness of the model was verified in an ECM scenario. Firstly, the process of the agent state transition was analyzed based on the CA method. Then, four state evolution strategies were studied, and the convergence performances of different parameters on the system were compared. Finally, the radar detection performance under different evolution strategies was simulated in distributed cooperative jamming scenarios. By comparing the detection probability of the system under different evolution strategies and the results of pulse compression output under different SNRs, the effectiveness of the interference signal was

verified. It can be concluded that the system achieves convergence and jamming quickly with an improved stability when the NA-AS strategy is adopted. However, the UAV communication is often limited by real-time transmission bandwidth. It is necessary to establish a suitable communication mechanism. Meanwhile, when multiple radiation sources appear in the actual environment, the UAV swarm needs to self-organize to sense the radiation sources and allocate interference resources. We will carry out the related research in future work.

**Author Contributions:** Methodology, Y.Z. and W.W.; software, Y.Z. and B.D.; validation, Y.Z. and B.D.; formal analysis, M.S.; investigation, B.R.; resources, W.W.; data curation, Y.Z.; writing—original draft preparation, Y.Z.; writing—review and editing, Y.Z. and D.S.; visualization, M.S.; supervision, D.S.; project administration, D.S.; funding acquisition, W.W. All authors have read and agreed to the published version of the manuscript.

**Funding:** This work was supported by the National Science Foundation for Young Scientists of China under Grant 62101558, and in part by the Research Foundation of National University of Defense University under Grant ZK21-38.

**Conflicts of Interest:** The authors declare no conflict of interest.

## Abbreviations

The following abbreviations are used in this manuscript:

UAV	Unmanned aerial vehicle
LQR	Linear quadratic regulator
EA	Electromagnetic agent
CA	Cellular automata
AS	All selection
NS	Neighborhood selection
ECM	Electronic countermeasure
SNR	Signal–noise ratio

## Appendix A

**Table A1.** The definition of mathematical symbols.

Mathematical Symbol	Definition
$G$	The communication topology diagram of the CA model
$E$	The set of communication edges between members
$D$	The degree matrix
$A(t)$	The adjacency matrix
$L$	The Laplacian matrix of the figure $G$
$x_i(t)$	The state of agent $i$
$u_i(t)$	The candidate set of the agent $i$
$\alpha$	The adjustment factor of the model
$N_n$	The number of agents in each sector
$N_c$	The number of communication sector
$P_r$	The radar receiving power
$P_t$	The radar transmitting power
$G_t$	The gain of the radar transmitting antenna
$G_r(\theta_t)$	The gain of the radar antenna in the target direction
$\sigma$	The radar cross section
$\lambda$	The wavelength of radar signal
$K_I$	The pulse accumulation correction factor
$K_C$	The pulse compression correction factor
$R$	The distance between radar and target
$L_s$	The loss of system
$P_{rj}$	The interference power received by the radar

**Table A1.** *Cont.*

Mathematical Symbol	Definition
$P_j$	The jammer transmitting power
$G_j$	The jammer transmitting antenna gain
$L_j$	The comprehensive loss of jammer
$F_r$	The radar center frequency
$T_r$	The pulse width
$B_w$	The chrip bandwidth
$B_r$	The bandwidth of receiver
$B_j$	The bandwidth of jammer
$P_{rn}$	The thermal noise power
$P_n$	The total noise power of the system
$T_0$	The standard room temperature
$F_n$	The noise figure
$P_{fa}$	The false alarm probability
$P_d$	The target detection probability
$S_{i\min}$	The minimum detectable signal power

**Appendix B**

*Appendix B.1. The Clear Air Atmosphere Attenuation*

The calculation process of the electromagnetic wave propagation attenuation model is as follows:

$$L_s = \gamma_0 r_0 + \gamma_w r_w \tag{A1}$$

where  $\gamma_0$  and  $\gamma_w$  represent the ground attenuation rates of oxygen and water vapor.  $r_0$  and  $r_w$  are the equivalent path lengths of oxygen and water vapor, respectively.

Suppose the path elevation angle is  $\theta$ , and the smaller and larger heights of the radiating source antenna and the reconnaissance receiver antenna are  $h_1$  and  $h_2$ , respectively.  $r_0$  and  $r_w$  can be calculated as follows:

$$r_0 = \begin{cases} \frac{h_0(e^{-\frac{h_1}{h_0}} - e^{-\frac{h_2}{h_0}})}{\sin\theta}, & 10^\circ \leq \theta \leq 90^\circ \\ \frac{\sqrt{a_e h_0} [F(\chi_1) e^{-\frac{h_1}{h_0}} - F(\chi_2) e^{-\frac{h_2}{h_0}}]}{\cos\theta}, & 0^\circ \leq \theta < 10^\circ \end{cases} \tag{A2}$$

$$r_w = \begin{cases} \frac{h_w(1 - e^{-\frac{h_1-h_2}{h_w}})}{\sin\theta}, & 10^\circ \leq \theta \leq 90^\circ \\ \frac{\sqrt{a_e h_0} [F(\chi'_1) - F(\chi'_2) e^{-\frac{h_1-h_2}{h_w}}]}{\cos\theta}, & 0^\circ \leq \theta < 10^\circ \end{cases} \tag{A3}$$

where  $h_0$  and  $h_w$  are the equivalent heights of oxygen and water vapor.  $a_e$  is the equivalent radius of the Earth.  $h_0$  and  $h_w$  can be calculated as follows:

$$a_e h_0 = \begin{cases} 6, & f \leq 63\text{GHz} \\ 6 + \frac{40}{(f - 118.7)^2 + 1}, & 63\text{GHz} < f \leq 350\text{GHz} \end{cases} \tag{A4}$$

$$h_w = h_{w0} [1 + \frac{3}{(f - 22.2)^2 + 5} + \frac{5}{(f - 183.3)^2 + 6} + \frac{2.5}{(f - 325.4)^2 + 4}], f < 350\text{GHz} \tag{A5}$$

where  $h_{w0}$  is the water vapor coefficient, and the value is 1.6 for sunny days and 2.1 for rainy days.

The calculation equation of  $F(\chi)$  can be represented as follows:

$$F(\chi) = \frac{1}{0.661\chi + 0.339\sqrt{\chi^2 + 5.51}} \quad (\text{A6})$$

$$\chi_i = \cos\theta[\sin\theta\tan^2\theta\sqrt{\frac{a_e}{h_0} + \sqrt{\frac{a_e}{h_0}\sin^2\theta + \frac{2h_i}{h_0} + \frac{h_i^2}{2a_e h_0}}}], (i = 1, 2) \quad (\text{A7})$$

$$\chi'_i = \cos\theta[\sin\theta\tan^2\theta\sqrt{\frac{a_e}{h_w} + \sqrt{\frac{a_e}{h_w}\sin^2\theta + \frac{2h_i}{h_w} + \frac{h_i^2}{2a_e h_w}}}], (i = 1, 2) \quad (\text{A8})$$

### Appendix B.2. Multipath Propagation Factor

In the process of calculating the multipath effect in the electromagnetic wave transmission process, it is first necessary to establish a vertical profile model of the actual ground on the transmission path from the radiation source to the reconnaissance receiver, and then analyze the possible arrival of the reconnaissance receiver antenna according to the electromagnetic wave reflection model. The radiation source reflects the signal. Finally, according to the electromagnetic characteristics of the reflecting surface and the transmission path, the reflection intensity and phase lag of the reflected signal are calculated, and then the composite signal of the direct wave and the reflected wave at the reconnaissance receiver is obtained. The calculation equation of multipath propagation factor is as follows:

$$F = f_d|\sqrt{1 + x_2 + 2xcos\alpha}| \quad (\text{A9})$$

where  $x = \frac{\rho_0\rho_s Df_r}{f_d}$  is the generalized reflection coefficient.  $\rho_0$  and  $\rho_s$  represent the electromagnetic reflection coefficient and roughness factor of the reflecting surface.  $D$  is the divergence factor of the reflecting surface.  $f_d$  and  $f_r$  represent the value of the amplitude of the pattern coefficient on the direct path and the reflected path, respectively.  $\alpha = \frac{2\pi\delta}{\lambda} + \varphi + \beta_r - \beta_d$  is the total phase difference between direct wave and reflected wave.  $\sigma$  is the path length difference between the direct wave and the reflected wave.  $\varphi$  is the phase angle of reflection coefficient.  $\beta_r$  and  $\beta_d$  represent the phase of the reflected and direct directions of the pattern factor.

## References

- Demirhan, M.; Premachandra, C. Development of an automated camera-based drone landing system. *IEEE Access* **2020**, *8*, 202111–202121. [\[CrossRef\]](#)
- Youn, W.; Ko, H.; Choi, H.; Choi, I.; Myung, H. Collision-free autonomous navigation of a small UAV using low-cost sensors in GPS-denied environments. *Int. J. Control. Autom. Syst.* **2021**, *19*, 953–968. [\[CrossRef\]](#)
- Shehzad, M.F.; Bilal, A.; Ahmad, H. Position & attitude control of an aerial robot (quadrotor) with intelligent pid and state feedback lqr controller: A comparative approach. In Proceedings of the 2019 16th International Bhurban Conference on Applied Sciences and Technology (IBCAST), Islamabad, Pakistan, 8–12 January 2019; pp. 340–346.
- Zhou, Y.; Rao, B.; Wang, W. UAV Swarm Intelligence: Recent advances and future trends. *IEEE Access* **2020**, *8*, 183856–183878. [\[CrossRef\]](#)
- Zhou, L.; Leng, S.; Liu, Q.; Wang, Q. Intelligent UAV swarm cooperation for multiple targets tracking. *IEEE Internet Things J.* **2021**, *9*, 743–754. [\[CrossRef\]](#)
- Wang, X.; Huang, T.; Liu, Y. Resource allocation for random selection of distributed jammer towards multistatic radar system. *IEEE Access* **2021**, *9*, 29048–29055. [\[CrossRef\]](#)
- Zhao, S.; Liu, Z. *Deception Electronic Countermeasure Applicable to Multiple Jammer Sources in Distributed Multiple-Radar System*; IET Radar, Sonar & Navigation: London, UK, 2021.
- Zhou, Z.; Rao, B.; Xie, X. The influence mechanism of UAV group on the detection performance of air defense radar. In Proceedings of the 2018 3rd International Conference on Automation, Mechanical Control and Computational Engineering (AMCCE 2018), Dalian, China, 12–13 May 2018; Atlantis Press: Beijing, China, 2018; pp. 338–343.
- Wang, L.; Liao, Y.; Luan, X. Research on UAV swarm interference based on improved invasive weed optimization algorithm. In *International Conference on Artificial Intelligence for Communications and Networks*; Springer: Cham, Switzerland, 2019; pp. 35–46.
- Cheng, J. *Modelling Spatial and Temporal Urban Growth*; Utrecht University: Utrecht, The Netherlands, 2003.

11. Devlin, J.; Schuster, M.D. Probabilistic cellular automata for granular media in video games. *Comput. Games J.* **2021**, *10*, 111–120. [[CrossRef](#)]
12. Mardiris, V.; Sirakoulis, G.C.; Mizas, C.; Karafyllidis, I.; Thanailakis, A. A CAD system for modeling and simulation of computer networks using cellular automata. *IEEE Trans. Syst. Man, Cybern. Part C (Appl. Rev.)* **2008**, *38*, 253–264. [[CrossRef](#)]
13. Byun, H.; Yu, J. Cellular-automaton-based node scheduling control for wireless sensor networks. *IEEE Trans. Veh. Technol.* **2014**, *63*, 3892–3899. [[CrossRef](#)]
14. Packard, N.H.; Wolfram, S. Two-dimensional cellular automata. *J. Stat. Phys.* **1985**, *38*, 901–946. [[CrossRef](#)]
15. Xie, G.; Lan, T.; Hu, X.; Li, Y.; Wang, C.D.; Yin, Y. A Distributed consensus protocol based on neighbor selection strategies for multi-agent systems convergence. *IEEE Access* **2019**, *7*, 132937–132949. [[CrossRef](#)]
16. Olfati-Saber, R.; Fax, J.A.; Murray, R.M. Consensus and cooperation in networked multi-agent systems. *Proc. IEEE* **2007**, *95*, 215–233. [[CrossRef](#)]
17. Ji, X.; Zhang, W.; Chen, S.; Luo, J.; Lu, L.; Yuan, W.; Hu, Z. Speeding up velocity consensus control with small world communication topology for unmanned aerial vehicle Swarms. *Electronics* **2021**, *10*, 2547. [[CrossRef](#)]
18. Ahmed, N.; Huang, H. Distributed jammer network: Impact and characterization. In Proceedings of the MILCOM 2009–2009 IEEE Military Communications Conference, Boston, MA, USA, 18–21 October 2009; pp. 1–6.
19. Wu, Q.; Zhao, F.; Wang, J.; Liu, X.; Xiao, S. Improved ISRJ-based radar target echo cancellation using frequency shifting modulation. *Electronics* **2019**, *8*, 46. [[CrossRef](#)]
20. Wu, Y.; Shen, X. A compound interference with distributed interference and false track interference for radar networking. In Proceedings of the 2012 6th Asia-Pacific Conference on Environmental Electromagnetics (CEEM), Shanghai, China, 6–9 November 2012; pp. 318–321.
21. Wang, F.; Li, H. Joint power allocation for multicarrier radar and communication coexistence. In Proceedings of the 2020 IEEE International Radar Conference (RADAR), Washington, DC, USA, 28–30 April 2020; pp. 141–145.
22. Zhang, S.; Zhou, Y.; Zhang, L.; Zhang, Q.; Du, L. Target detection for multistatic radar in the presence of deception jamming. *IEEE Sens. J.* **2021**, *21*, 8130–8141. [[CrossRef](#)]